*EVS30 Symposium*
*Stuttgart, Germany, October 9 - 11, 2016*

# Assessment of thermal comfort and energy efficiency of alternative ventilation concepts

P. Lange[1*], Dr. D. Schmeling[1], T. Dehne[1], Dr. M. Konstantinov[1], Dr. J. Bosbach[1]
[1]*German Aerospace Center (DLR), Institute of Aerodynamics and Flow Technology, Göttingen, Germany*
[*]*Pascal.Lange@dlr.de*

**Abstract**

We compared state of the art mixing ventilation (MV) to a novel ventilation concept based on displacement ventilation (HV). Hereto, we conducted experimental and numerical investigations addressing thermal comfort as well as ventilation and energy efficiency in a generic car mock-up. We considered winter, summer and spring/fall conditions. Concerning the ventilation efficiencies, HV performed comparable or better than MV. Comfort benefits are expected from equivalent temperature measurements for spring/fall and summer conditions. None of the systems was able to provide comfortable conditions in the winter scenario, however, MV revealed the best cooling efficiency, while HV provided the best heating efficiency.

*Keywords: air conditioning, thermal management, efficiency, EV, research.*

## 1 Introduction

The Next Generation Car (NGC) project is a large-scale project developing new electrical vehicle concepts and the related technologies. It covers six research and development domains: the overall vehicle concepts, the lightweight body design, advanced powertrain, efficient energy management, mechatronic chassis and vehicle intelligence. The project has a holistic approach focusing on integrated development of technologies, methods and tools for future cars. Within this project, we focus on novel ventilation concepts, which are investigated numerically and experimentally. Thereby, the thermal comfort, the local ventilation efficiency and the global energy efficiency are studied in detail.

The improvement of the restricted cruising range of future electric vehicles (EVs) is a key challenge for car manufactures and scientists to commercialize modern EVs. To optimize the energy consumption of EVs, numerous factors have to be taken into account. In this context the climatization of the interior has to be mentioned, being one of the most range limiting systems. Under extreme winter and summer conditions, up to 50 % of battery power are required for heating or cooling the car cabin [1]. This is one reason to investigate novel ventilation systems for conditioning a car cabin in an efficient way. The increasing importance of autonomous driving is another reason for novel ventilation systems. In future EVs the front seats will be rotatable, so that dashboard based ventilation will not be able to provide proper ventilation of the seated passengers. Hence, vertical ventilation concepts could be a solution to provide the interior with fresh and well tempered air. Meanwhile, the passenger comfort may not suffer from all efforts to reduce the energy consumption. It is influenced by thermal conditions as well as by air quality, among other things. At DLR, studies on vertical ventilation concepts for passenger aircraft cabins, such

as cabin displacement ventilation (CDV), ceiling based cabin displacement ventilation (CCDV) and hybrid ventilation (HV) as a combination of CDV and CCDV have shown significant benefits concerning heat removal efficiency and reduced draft risk [2]. The first results of the experimental and numerical investigations of novel ventilation concepts in the generic car mock-up (GCC) demonstrate the potential of optimized thermal passenger comfort and an efficient use of energy [3],[4]. In the framework of NGC, CDV, CCDV and HV were analyzed experimentally with local temperature and velocity probes and compared to mixing ventilation (MV). It turned out that presumably only HV is able to provide a comfortable thermal environment under spring/fall conditions. Therefore, we focus in the current study on the comparison of hybrid ventilation as a vertical ventilation system with dashboard based mixing ventilation. Furthermore, we complement the previous investigations by considering summer and winter scenarios, i.e. extreme cooling and heating conditions in addition to the spring/fall case. This is achieved by using a jacket heating/cooling system for the GCC. Further, equivalent temperature measurements are employed as an integral measure for thermal passenger comfort. Finally, air quality is considered by measuring ventilation efficiency using tracer gas techniques.

# 2 Test facilities and ventilation concepts

## 2.1 Generic car cabin as a test facility

Within the framework of the NGC-project, a dedicated full-scale generic car cabin test facility was developed and set-up at the DLR in Göttingen, see Fig. 1a). It is basically made of aluminum profiles and acrylic glass (PMMA). The interior of the GCC corresponds to the dimensions of standard mid-range industrial cars, for further information see [3]. A thermal insulation of 5 cm extruded polystyrene rigid foam was applied to the mock-up to decouple the cabin interior from the ambient and to provide stationary boundary conditions. This passive insulation was used during the experimental investigations of the ventilation efficiency.

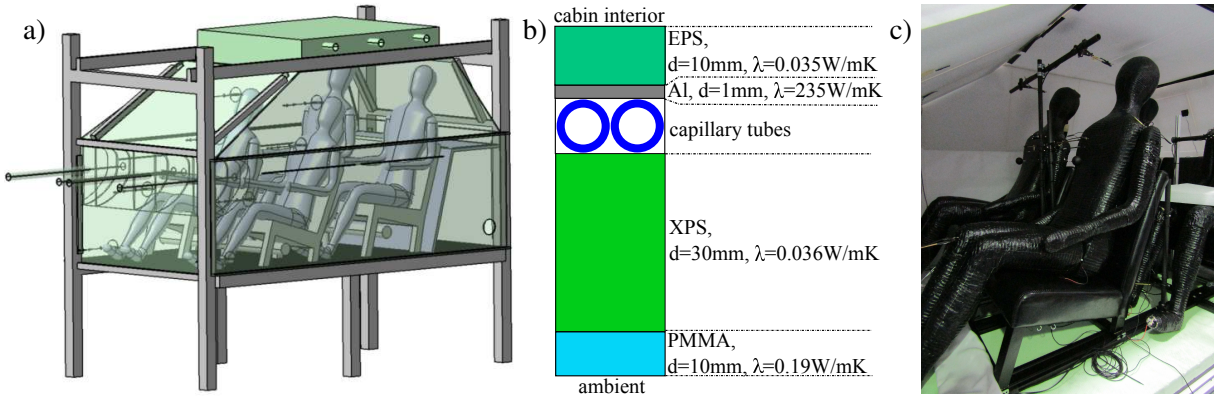


Figure 1: a): CAD of the generic car cabin test facility, b) cabin structure with insulation as well as jacket heating/cooling, c) picture of the thermal manikins seated in the GCC.

To simulate different environmental conditions (winter, spring/fall and summer), the structure of the GCC was enhanced by a jacket heating/cooling system, which is shown schematically in Fig. 1b). A 30 mm thick layer of extruded polystyrene rigid foam (XPS) is followed by the capillary tubes for supplying temperature controlled water. These tubes are connected to aluminum sheets, which are used to achieve a homogeneous temperature distribution. Subsequently, an insulation of 10 mm expanded polystyrene rigid foam (EPS) is attached to the aluminum sheets to simulate the vehicle lining and thus to allow a temperature profile on the inner surfaces. Fig. 1c) shows the thermal manikins, also called thermal passenger dummies (TPDs), seated in the GCC. These models of the human body are made of non-combustible foam equipped with a heating wire to simulate the thermal behavior of passengers. By using an external power supply, each thermal manikin provides a constant heat flux of 75 W during the experimental investigations.

## 2.2 Investigated ventilation concepts

### 2.2.1 Mixing ventilation

The full-scale generic car cabin allows to integrate different ventilation concepts with a high degree of flexibility. Nowadays, mixing ventilation (MV, see Fig. 2) is state of the art for the ventilation of a car cabin. A high degree of mixing of incoming fresh air and recirculated cabin air is characteristic for this type of ventilation. The air enters the passenger compartment with a high discharge momentum through supply tubes in the dashboard. After circulation, the air leaves the cabin through outlets in the luggage

compartment. Due to the large momentum of inflowing air, high velocities occur. Accordingly, the risk of discomfort caused by draughts is tremendous. As a simplification, the mixing ventilation system of the GCC was embodied by four circular air inlets, embedded in the front panel. Hence, undisturbed circular air jets in longitudinal car direction were generated. This configuration is similar to fully open air inlet grills in a common car. Since no air supply tubes are integrated at foot level, the air inlet configuration of MV corresponds to those under summer conditions.

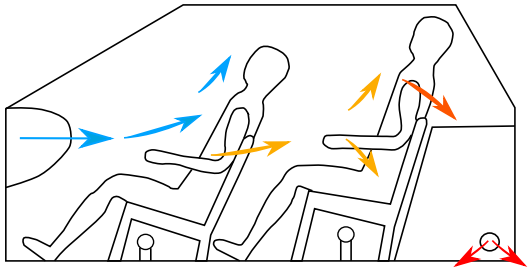

Figure 2: Sketch of MV as an investigated ventilation system, blue arrows denote fresh incoming air and red ones the warm air leaving the cabin.

#### 2.2.2 Hybrid ventilation

In addition to dashboard MV, a novel, vertical ventilation concept, called hybrid ventilation (HV), is discussed in this article. Fig. 3 shows the functional principle of HV. The passenger compartment is supplied with fresh air at low momentum through air inlets at floor and ceiling level using permeable air ducts. Under summer conditions, the supposedly colder fluid descends and generates a "lake" of fresh air at floor level. Due to buoyancy, the air heats up and rises at the heat loads. The warm air finally leaves the cabin through outlets at ceiling level. Due to the very low flow velocities, the risk of comfort critical draughts is minimized. Early studies regarding pure cabin displacement ventilation revealed temperature stratifications from ankle to head level of up to 7 K. Using the air inlet configuration of HV, the temperature stratifications have been strongly reduced [3]. Furthermore, HV provides the opportunity to optimize local zones of discomfort by adjusting the inlet temperatures and volume flow rates.

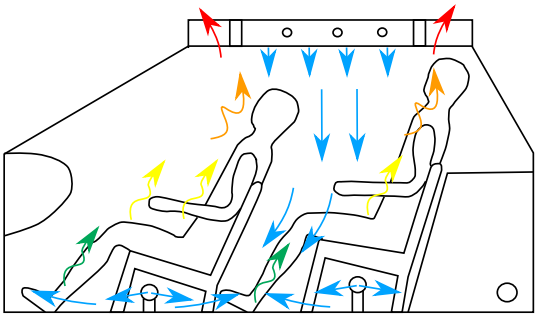

Figure 3: Sketch of HV as an investigated ventilation system, blue arrows denote fresh incoming air and red ones the warm air leaving the cabin.

## 3 Measurement techniques

### 3.1 Experimental analysis of passenger comfort

#### 3.1.1 Local temperature and velocity probes

In order to evaluate the thermal environment of the passenger air temperatures, surface temperatures and air velocities were monitored. In total, more than 70 platinum resistance temperature detectors (RTDs) were used to capture the boundary conditions as well as surface and fluid temperatures at selected positions within the GCC. In the range of the investigated temperatures, these probes provide an accuracy better than $\pm 0.15$ °C (1/3 DIN B) [5]. As Fig. 4a) depicts, several probes were located in the air supply tubes as well as in the air outlets to monitor temperatures of the in- and outflowing air. Further, eight probes were used to measure the temperature of the outer surface of the generic car cabin. Another twelve probes captured the temperature of the surrounding in a distance of 50 mm. At the side walls,

floor, ceiling, front and rear panels 24 RTDs monitored the inner surface temperatures within the GCC.

In order to acquire comfort relevant fluid velocities and temperatures in the vicinity of the TPDs, omni-directional velocity and temperature probes (OVPs) were installed on sensor arrays in the first seat row, see Fig. 4b). As indicated in Fig. 4a), the probes were positioned at ankle, knee, chest, and head level (50 mm apart from the surface of the TPD). This arrangement offers the opportunity to evaluate temperature and velocity stratifications near the thermal manikins. The accuracy of these probes amounts to $\pm$0.02 m/s for velocity and $\pm$0.2 K for temperature [6].

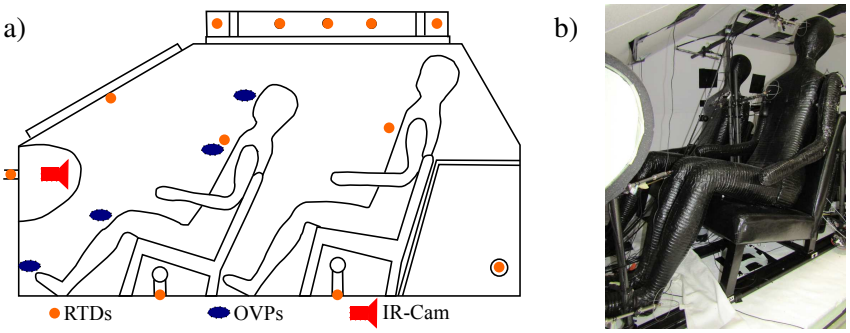


Figure 4: a) probe positions inside the GCC, b) temperature and velocity probes in vicinity of the manikin.

### 3.1.2 Infrared thermography

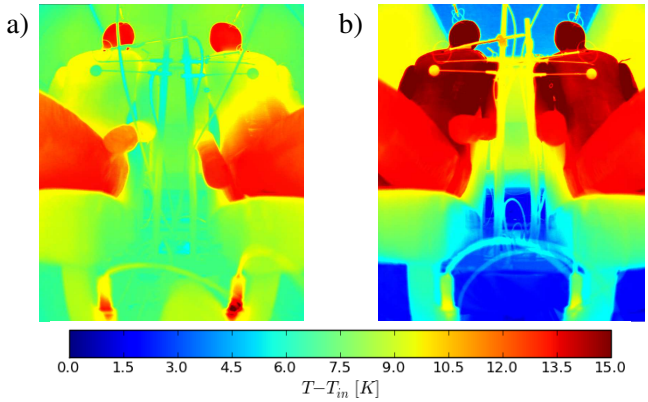


Figure 5: Infrared image with surface temperatures of the manikins and cabin interior: a) MV, b) HV.

To determine the surface temperatures of the TPDs and the cabin interior, infrared (IR) thermography was used. As an example, Fig. 5 depicts two infrared views of the heated thermal manikins and parts of the surrounding walls for MV (Fig. 5a)) and HV (Fig. 5b)). These images were taken under steady conditions at a volume flow rate of $q_V$=28 l/s, an inlet temperature of $T_{in}$=21.1 °C and an ambient temperature of $T_{am}$=20.7 °C. The temperatures in the torso region of the TPDs are significantly lower for MV as compared to HV, which indicates a much higher amount of forced convection due to the high discharge momentum of the incoming air at MV. Regarding the surface temperatures of the interior, lower temperatures above the head level and in the bottom part can be recorded for HV. This is caused by the ceiling air inlets and the air ducts under the seats, respectively. IR-images of the driver-TPD were also used to calculate equivalent temperatures ($T_{eq}$). Therefore, an IR-camera was installed in the dashboard of the GCC, see Fig. 4a). Using this camera, high-definition infrared images with a resolution of 1280 x 960 pixel were taken to investigate mean surface temperatures of different body parts of the TPD in the following. Detailed information on capturing and evaluating equivalent temperatures is given in section 3.1.3.

### 3.1.3 Equivalent temperature

The thermal passenger comfort in car cabins is influenced by the interaction of a variety of parameters, such as air temperature, air velocity, surface temperatures, thermal radiation. Accordingly, the acquisition of single thermal parameters is often insufficient for the evaluation and quantification of the thermal

passenger comfort. The equivalent temperature ($T_{eq}$) expresses the effect of all thermal influences combined by a single quantity. Thereby $T_{eq}$ can be interpreted as the temperature of an imaginary enclosure with the mean radiant temperature equal to air temperature and still air in which a person has the same heat exchange with the surrounding as under real conditions, see [7]. To calculate $T_{eq}$, a TPD was calibrated in a temperature controlled chamber. After stable thermal conditions have been reached, the mean surrounding temperature in the calibration chamber ($\langle T_{Ch} \rangle$) was calculated, which indicates $T_{eq}$. Using IR-thermography, mean surface temperatures ($\langle T_{Surf} \rangle$) of 14 body parts of the TPD were measured, see Fig. 6a). The calibration curves of the observed upper body and the lower body parts are shown in Fig. 6b) and c), respectively. All of them reveal almost linear dependencies of the respective surface temperatures $T_{Surf}$ from mean surrounding temperature $\langle T_{Ch} \rangle$ with a slope close to unity. The calibration curves allow to calculate $T_{eq}$ on the basis of the surface temperatures for TPD operated under constant heat flux conditions. The accuracy is mainly determined by the homogeneity of the temperature in the chamber and increases with rising temperatures. At the highest surface temperature ($\langle T_{Surf} \rangle = 42.1°\text{C}$), an uncertainty of $\Delta T_{eq} = 0.42K$ was obtained.

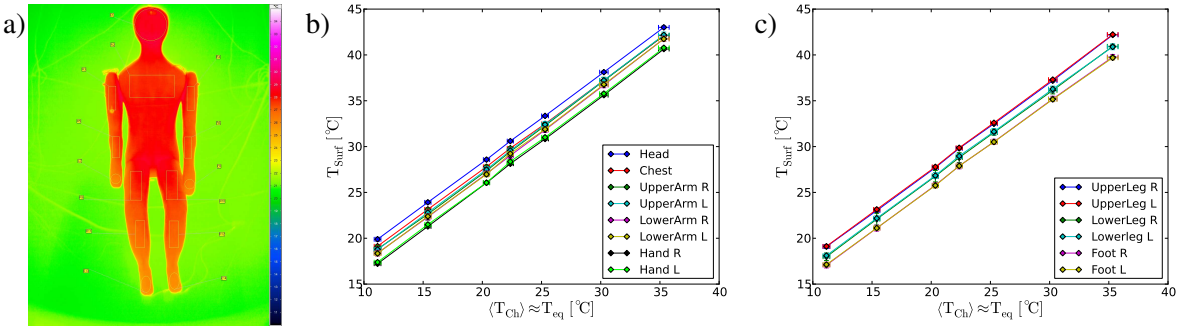


Figure 6: a): Infrared view with mean surface temperatures of a TPD in a calibration chamber, b) calibration curves of the upper body, c) calibration curves of the lower body.

### 3.1.4 Ventilation efficiency

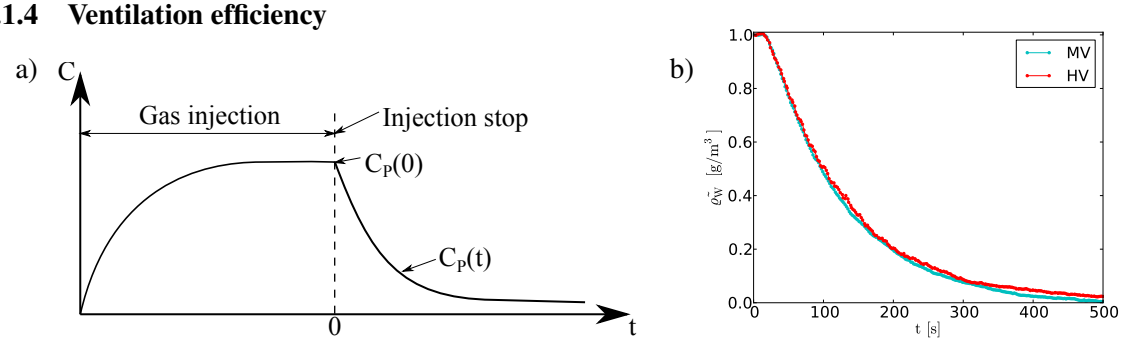


Figure 7: a) principal approach of the step-down method b) decay curves of different ventilation concepts.

Besides thermal conditions in car cabins, air quality determined by e.g. the mixing behaviour and the distribution of pollutants, are essential for the passenger comfort and health as well. Accordingly, different figures of merit for the ventilation efficiency were investigated for MV and HV, i.e. the local mean age of air as well as the local and global ventilation efficiency, see [8]. The local mean age of air ($\tau_P$) is defined as the mean time required by the supply air to reach a point $P$ in a room. The mathematical relationship between the local age of air and the nominal air exchange rate quantifies the local air quality and is called local ventilation efficiency ($\varepsilon_P$). The global ventilation efficiency ($\eta_a$) relates the spatially averaged mean age of air in the compartment to the nominal air exchange rate. Thus, it is a measure for the fraction of still waters. All the ventilation efficiency measurements were conducted using the tracer gas technique in a step-down measurement approach. Water was used as tracer gas to facilitate the detection. An example sequence of a step-down method is shown in Fig. 7a). The GCC was enriched with moist air until steady local concentrations were observed. After stopping the tracer injection ($t = 0$), the gas concentration decayed as a result of the air exchange. Using humidity sensors, the decay curves were monitored at selected positions near the TPDs as well as in the air in- and outlets. Fig. 7b) shows the decaying humidity concentration curves ($\varrho_W$) at the air outlet for MV and HV. The recorded curves were used to calculate the local mean age of air and the local ventilation efficiency according to [8]. The global ventilation efficiency was calculated following the description of [9]. Condensation effects within

the GCC were avoided by choosing the appropiate tracer gas concentrations and temperature levels. For additional information about tracer gas techniques and tracer injection methods see [10].

### 3.2 Numerical comfort simulation

In order to give an insight into the flow phenomena and temperature distribution within the GCC, numerical investigations were conducted. The Reynolds-averaged Navier-Stokes (RANS) equation with the Boussinesq approximation was solved with second order linear upwind schemes for turbulence, scalar, vector and radiation fields provided in OpenFOAM. Equations were discretized and integrated on a hybrid structured/unstructured mesh consisting in total of 10 million cells, which were generated with StarCCM+. The thermal boundaries were resolved by means of five wall layers and wall distances in wall units of the grid points next to the wall of $y+ < 1$ in 92 % of the wall cells.
HV and MV were examined using the same thermal boundary conditions as in experiment, see Table 1. The total heat flux of the manikins was prescribed to $Q_{total}$=75 W. The conducted turbulent flow simulations include the computation of heat radiation based on a Discrete Ordinates Model (DOM) with 40 rays. The steady state simulations were carried out with a "buoyantBoussinesq" solver of OpenFOAM provided by the Engys GmbH, which integrates the RANS equations together with the k-$\omega$/SST model. To correctly depict the wall temperatures, the calculation using isothermal boundary conditions was carried out at first. As a result of this calculation, the wall heat fluxes were determined and used later as new wall thermal boundary conditions. The temperature is distributed qualitative correctly in terms of quality on the wall.

## 4 Results

If not stated otherwise, all results are given for a volume flow rate of 25 $\mathrm{m}^3/\mathrm{h}/\mathrm{PAX}$ [11], corresponding to 28 l/s for four passengers. To determine the scaling behaviour, two further volume flow rates (36 l/s, 44 l/s) were considered for the investigation of the ventilation efficiency. To simulate different seasonal conditions in the experiments, the temperature difference between incoming air and aluminum sheet has been varied systematically. Hereto, the temperature level of the incoming air had to be shifted for technical reasons up to values in the range between 22-28 °C, resulting in cabin temperatures too high for operational conditions. However, since our TPDs were operated with constant heat flux, the temperature differences relative to the incoming air remained almost unaffected. Hence, the real boundary conditions have been corrected for each scenario (winter, summer, spring/fall) with an offset temperature that results in comparable mean (averaged over all positions and ventilation systems) equivalent temperatures. The corrected boundary conditions (inlet temperature ($T_{in}$) and aluminum sheet temperature ($T_A$)) for the investigation under different environmental conditions are given in Table1.

Table 1: Corrected boundary conditions of the investigated winter, spring/fall and summer cases.

| | Winter | Spring/Fall | Summer |
|---|---|---|---|
| $T_{in}$[°C] | 24.8 | 19.9 | 14.0 |
| $T_A$[°C] | 6.9 | 19.9 | 29.1 |

### 4.1 Numeric results

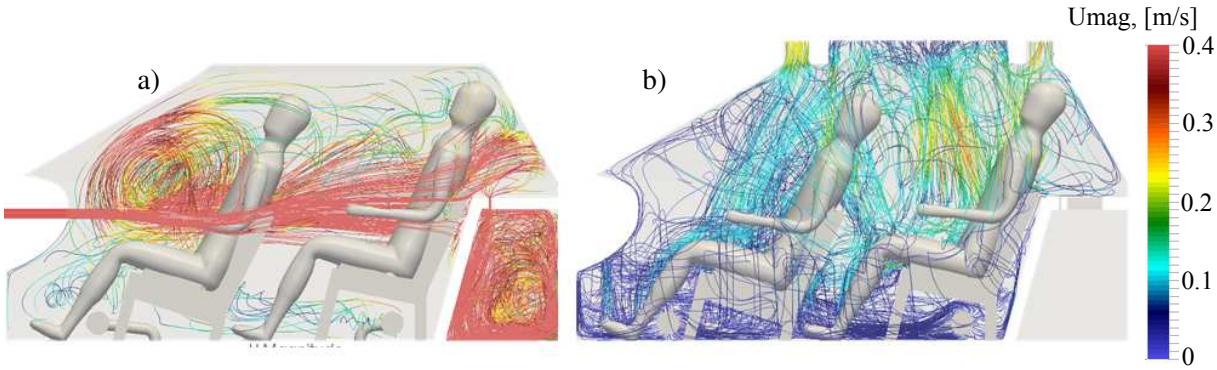


Figure 8: Velocity-colored streamlines within the GCC for a) MV, b) HV under spring/fall conditions.

As the thermal parameters of the different ventilation systems are the same for each case, their performance is solely determined by the applied volume flow and momentum flux distribution. CFD provides

a very useful means to get insight into the three-dimensional flow structure of the resulting mixed convective flow states. Fig. 8 depicts the velocity streamlines in the cabin for MV and HV under spring/fall conditions. Clearly, the characteristic difference of the two flow states can be recognized. At MV the fresh enters the cabin with high velocity, generating horizontal air jets that move through the whole cabin. The flow at HV is dominated by the convection occurring in vertical direction between heated thermal dummies and cold ceiling outlets. Noticeable is the apparent high degree of mixing even at HV. At MV, mixing is system inherent, however Fig. 8a) reveals the actual path of the fresh air jets which hit the passenger dummies and result in an increase amount of forced convection in the upper cabin. Fig. 9 shows a similar visualization with temperature colored streamlines, revealing the temperature distribution in the cabin. Clearly, the fresh air lake at floor level and the unstable thermal stratification at the ceiling, which drive the cabin flow at HV can be seen in Fig. 9b). At MV, the temperature distribution is much more homogeneous, however the reduced surface temperatures of the TPDs indicate the increased amount of forced convection by the elevated fluid velocities.

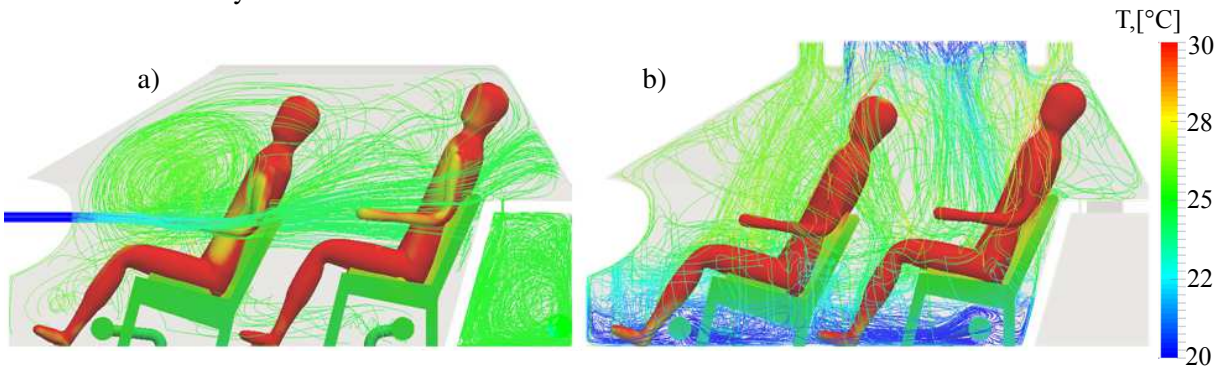


Figure 9: Temperature-colored streamlines and surface temperatures for a) MV, b) HV under spring/fall conditions.

## 4.2 Local and global ventilation efficiency

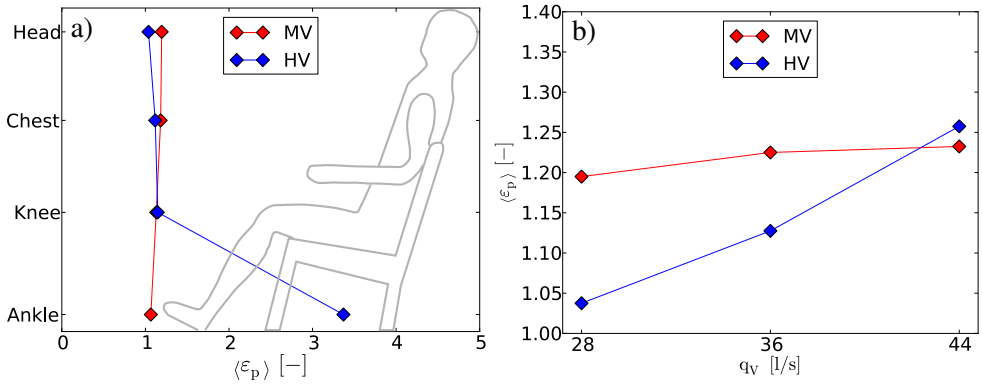


Figure 10: a) Local ventilation efficiency in the proximity of the TPDs for MV and HV at a volume flow rate of 28 l/s, spatially averaged over four seating positions, b) local ventilation efficiency at head level for MV and HV at different volume flow rates, spatially averaged over four seating positions.

Before looking at the achievable thermal comfort and energetic efficiency, we would like to discuss the ventilation efficiency first as a necessary precondition for implementation of novel concepts. Fig. 10a) depicts the the local ventilation efficiency for the two investigated ventilation concepts, measured at different heights near the TPDs. These measurements were performed at a volume flow rate of 28 l/s and the calculated values are spatially averaged over the four passengers within the GCC. At all sensor positions, MV reveals a homogeneous local ventilation efficiency of approximately 1.0, which means that $\tau_P$ at each measuring point is at least equal to $\tau_P$ at the air outlet. Accordingly, the time required to refresh the air in the vicinity of the TPDs is equal to or shorter than the time nominally needed to replace the air in the whole compartment. The values of HV at knee and chest level are similar to MV, whereas the local ventilation efficiency at ankle position rises up to 3.4. The reason for that lies in the air inlet configuration of HV. Due to the supplied air at floor level, the air is replaced faster by fresh air which results in increasing values of $\varepsilon_P$. As shown in Fig. 10a), the local ventilation efficiency of HV at head level is slightly lower as compared to MV.
As already mentioned, the air exchange along with contaminant removal is essential for air quality and passenger health within a car. Consequently, the local ventilation efficiency at breathing level is an

important quantity to evaluate the air quality. To examine the behaviour of MV more closely, Fig. 10b) unveils $\varepsilon_P$, spatially averaged over four head positions for three different volume flow rates. As indicated in Fig. 10a) for the two investigated ventilation concepts, all values of $\varepsilon_P$ are clearly larger than 1.0. For MV, the local ventilation efficiency ($\varepsilon_P \sim 1.2$) remains approximately the same with increasing volume flow rate. At HV, a rising $\varepsilon_P$ from 1.04 to 1.26, with increasing volume flow rate can be observed. Here, at a volume flow rate of 44 l/s the local ventilation efficiency of HV is 2.4 % higher compared to MV.
To describe the ventilation efficiency of a system in its entirety, the global ventilation efficiency was measured using tracer gas techniques as well. Fig. 11 shows the global air change efficiency ($\eta_a$) for the different ventilation scenarios and volume flow rates. The calculated values vary between 51 % and 58 % for the two ventilation concepts.

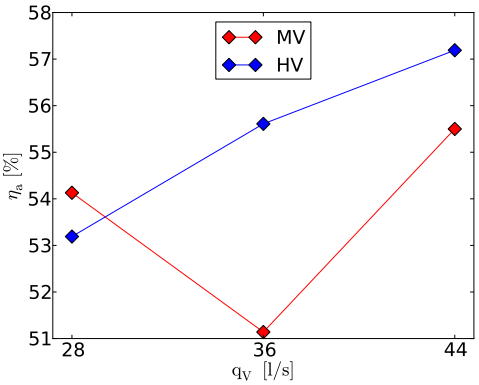


Figure 11: Global ventilation efficiency for MV and HV at different volume flow rates.

For HV, an increasing global ventilation efficiency of 53.1 % to 57.2 % was observed. Except for the value at 28 l/s, the global air change efficiency of HV is significantly higher as compared to MV. For MV at the lowest volume flow rate, $\eta_a$ is about 1 % higher as compared to the value of HV. However, for MV, a decrease of the global ventilation efficiency of 3 % was found at a volume flow rate of 36 l/s. For the highest volume flow, $\eta_a$ increased to 54.5 %.
In summary, despite the low momentum of the inflowing air at HV, only slightly lower values of the local ventilation efficiency were detected at breathing level. Adjusting the volume flow distribution for HV might improve the performance of the hybrid ventilation system, especially at head level. For the novel ventilation concept, it should be noted that the exchange of used air is mainly achieved by thermal convection of the TPDs. However, HV shines out with a good global ventilation efficiency for 36 l/s and 44 l/s.
In summary, there are new objections against the implementation of HV in terms of air quality according to our measurements.

## 4.3 Local fluid temperatures and flow velocities

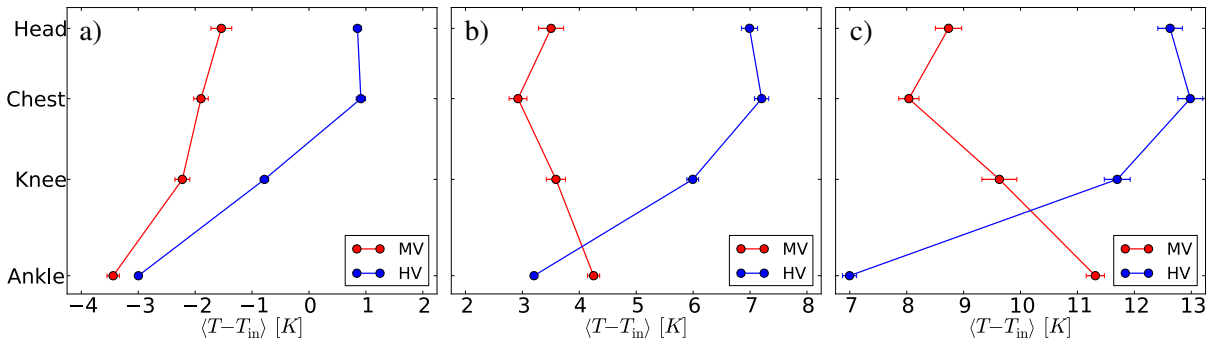


Figure 12: Mean fluid temperatures and standard deviations at different heights in the vicinity of the TDPs. Comparison of HV and MV as ventilation systems at a volume flow rate of 28 l/s for a) winter, b) spring/fall and c) summer condition.

To evaluate the thermal environment in the proximity of the TPDs, Fig. 12 shows the temperature stratifications for winter, spring/fall and summer conditions. The temperatures are given relative to the mean temperature of the incoming air. The mean values and standard deviations are calculated by temporal averaging at each sensor position and subsequent spatial averaging over two seat positions (driver and co-driver). For all investigated environmental conditions, MV shines out with small temperature stratifications from ankle to chest. Under winter conditions, for HV the mean fluid temperatures increase from

-3 K to 1 K. Accordingly, the maximum vertical temperature difference of 4 K for a comfortable climate in car cabins is adhered to [11]. However, the higher absolute temperature level for HV indicates a better heating efficiency under winter conditions. To ensure comfortable thermal conditions in the spring/fall and summer case, it is necessary to remove heat by the ventilation systems. The temperature differences between ankle and head are smaller for MV compared to HV, see Fig. 12. This means that MV is more suitable for cooling the GCC. Regarding the thermal comfort, for HV the temperature stratification from head to ankle increases from 3.6 K (spring/fall case) to 5.5 K (summer case). Especially the latter value is comfort critical, following the statements given in [11]. Adjusting the volume flow rate or the temperature of the incoming air could result in improvements concerning temperature stratifications for HV. The temperature fluctuations are also important for evaluating thermal comfort of ventilation systems. Here, maximum fluctuations for MV of 0.2 K were observed, which have a predictably minimal influence on the thermal passenger comfort. For HV, the standard deviations are significantly lower as compared to MV.

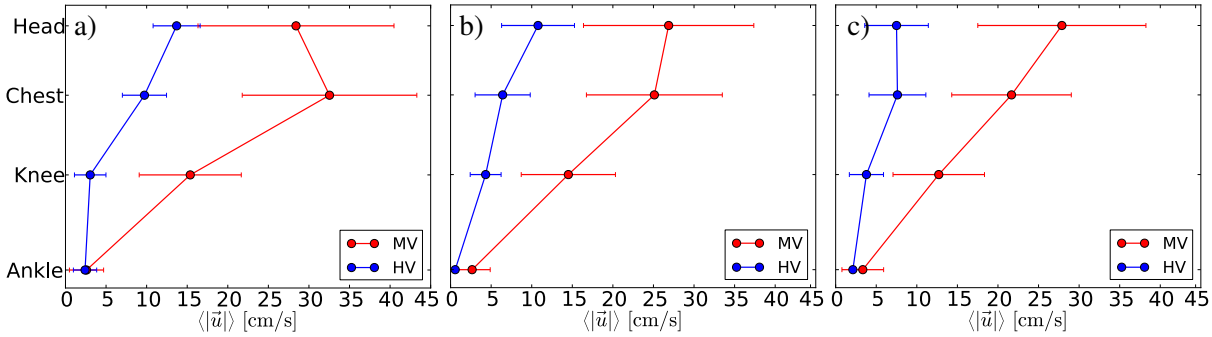


Figure 13: Mean fluid velocities and standard deviations at different heights in the vicinity of the TDPs. Comparison of HV and MV as ventilation systems at a volume flow rate of 28 l/s for a) winter, b) spring/fall and c) summer condition.

Besides local temperatures, flow velocities are a further indicator for evaluating the thermal passenger comfort in car cabins. The measured mean fluid velocities and standard deviations for MV and HV under winter, spring/fall and summer conditions are shown in Fig. 13a) - c). For all investigated cases, MV reveals significantly higher mean velocities than HV due to the high kinetic energy of the inflowing air. For the winter case, maximum mean velocity (32 cm/s) and velocity standard deviation (12 cm/s) were observed at chest level, which exceed the comfort limiting value of 30 cm/s as defined by [11]. As Fig. 13 depicts, for HV much lower mean velocities and standard deviations could be detected. Furthermore, the velocity distribution from ankle to head is more homogeneous as compared to MV.

## 4.4 Equivalent temperatures

While the point wise measurements of fluid temperatures and velocities discussed in the previous section only allow indirect estimates, this section is dedicated to equivalent temperature as an integral means to judge on the achievable thermal passenger comfort. The equivalent temperature is often used as a measure to quantify the thermal comfort in car cabins. To evaluate this quantity, high resolution infrared images of the driver-TPD were recorded through the dashboard of the GCC.

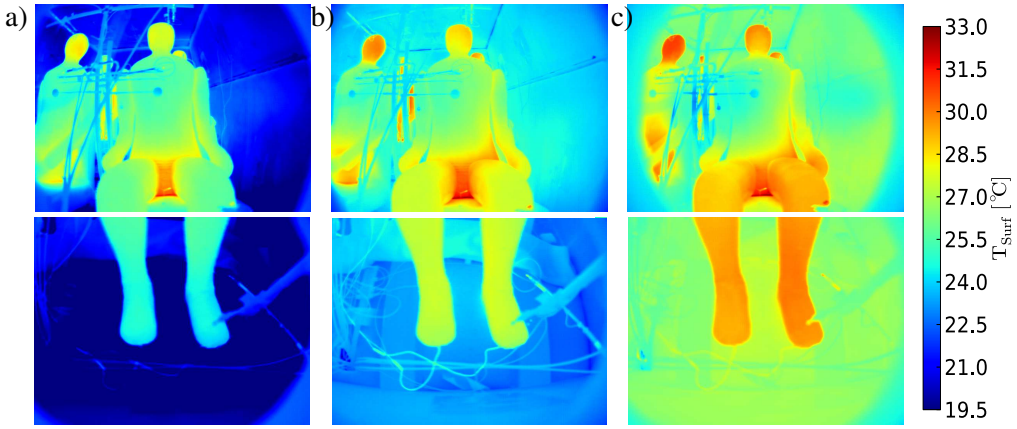


Figure 14: IR images within the GCC for MV under a) winter, b) spring/fall and c) summer conditions.

Fig. 14 and 15 depict infrared images of the upper body as well as the legs for MV and HV under winter (a)), spring/fall (b)) and summer (c)) conditions. The higher amount of forced convection for MV results

in lower surface temperatures at the upper body of the TPD compared to HV. For MV, regions where the incoming jets hit the TPD (upper arms, chest and abdominal region) are colder in contrast to the other body parts. Furthermore, the temperatures of the upper body and legs are higher under summer conditions than under winter conditions. For HV in the summer case, the highest temperatures of the upper body were detected. Additionally, due to the ceiling air inlet, lower surface temperatures above the head were observed for HV. The infrared images for HV under spring/fall and summer conditions also show lower temperatures of the legs and feet in contrast to MV. The air inlets mounted below the seats provide a "lake" of fresh air, which is the reason for the lower temperatures in the bottom part.

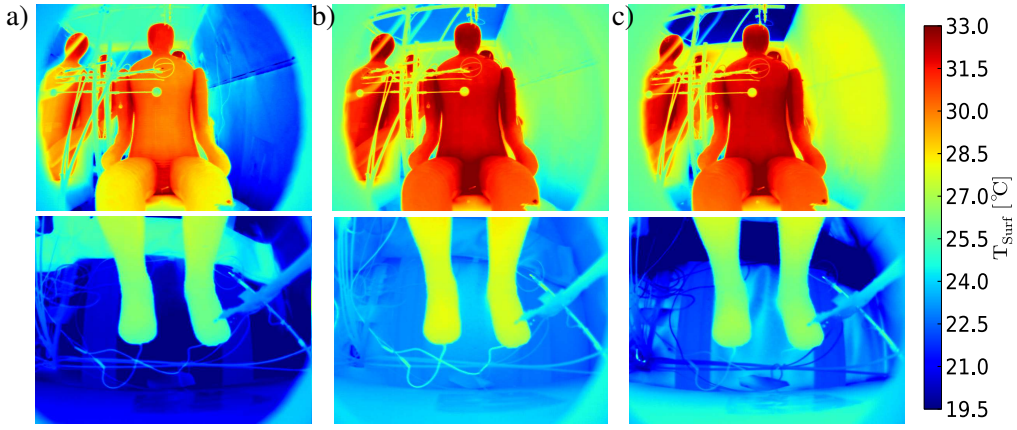


Figure 15: IR images within the GCC for HV under a) winter, b) spring/fall and c) summer conditions.

The calibration curves (see, Fig. 6a) and b)) combined with the surface temperatures, provided by infrared images, were used to calculate equivalent temperatures. The results are presented in Fig. 16 for winter (a), spring/fall (b) and summer (c) conditions. According to [7], empiric comfort zones, ranging from too cold (1) via neutral (3) to too warm (5), served as evaluation criteria. The evaluated body segments are determined by the optically accessible surface areas of the driver-TPD.

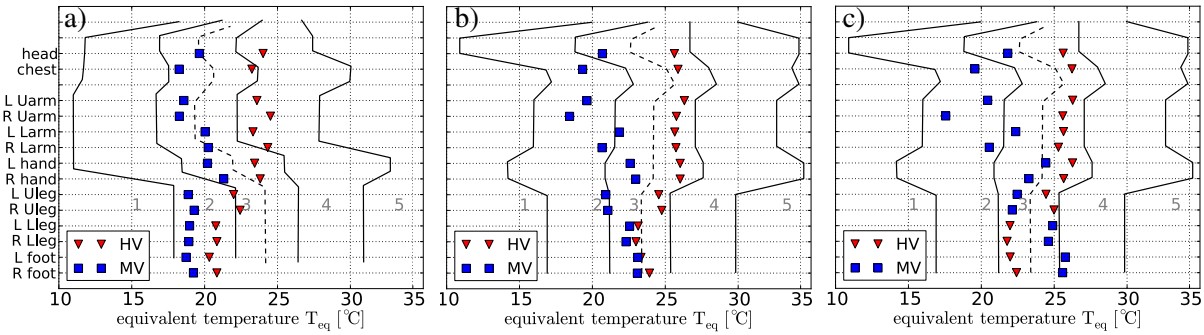


Figure 16: Equivalent temperature results of driver-TPD for a) winter, b) spring/fall c) summer condition.

While the air inlet temperatures are identical for both investigated ventilation systems, the calculated equivalent temperatures vary strongly between HV and MV, especially on the upper body parts (see Fig. 16). In the winter case, comfortable thermal conditions only in the upper body part, i.e. from head to hands. In contrast, the rising air due to buoyancy results in too warm temperatures of these body segments for HV. The equivalent temperatures at the lower body are too low for both investigated ventilation concepts. In case of MV, foot nozzles could possibly improve the thermal comfort at the lower body parts. Similarly, in case of HV, a better thermal comfort could be reached by adjusting the air inlet temperatures as well as volume flow rates. However, these results suggest that the hybrid ventilation system is much more efficient for heating the car cabin. The distribution of the equivalent temperatures at spring/fall conditions (see Fig. 16b)) show that the highest thermal comfort is achieved using HV. Again, on account of the high momentum induced by the air jets, low equivalent temperatures at the upper body were detected for MV. Under summer conditions, analogous results to the spring/fall condition were observed. MV reveals the highest cooling efficiency indicated by lower mean equivalent temperatures, however, HV provides more comfortable equivalent temperatures.

## 5 Conclusion

A novel vertical ventilation concept, called hybrid ventilation (HV), was studied in comparison to a dashboard ventilation system (mixing ventilation MV) in a GCC. The results of the experimental investigations and numerical simulations addressing the thermal comfort and the ventilation efficiency within

a generic car cabin (GCC) were presented and discussed. The air inlet configuration of HV is based on permeable air ducts mounted below the seats and at the ceiling. Using tracer gas measurement methods, local and global ventilation efficiencies were analyzed. Different environmental conditions (winter, spring/fall and summer conditions) were investigated using a jacket heating/cooling system in the GCC. Local temperature and velocity probes were used to measure comfort relevant fluid temperatures and flow velocities in the proximity of thermal passenger dummies (TPD). The latter were used to provide the thermal impact of real passengers and simultaneously as a means to determine equivalent temperatures.
Regarding the comfort relevant fluid velocities and temperatures, MV unveils a homogeneous temperature distribution inside the GCC. However, high air velocities and turbulence levels were detected. HV, as a novel vertical ventilation concept, is characterized by a homogeneous flow velocity distribution, where comfort critical vertical temperature stratifications could be observed, especially for cooling cases (at summer conditions). Concerning the ventilation efficiency, HV performs comparably good or even better than MV, although the air exchange is mainly based on thermal convection due to the buoyancy of the TPDs. Depending on the volume flow rate, the local ventilation efficiency at head level and the global ventilation efficiency are higher as compared to MV. These findings indicate that for HV further fine-adjustments of the volume flow split could lead to a more efficient ventilation. Concerning the equivalent temperatures at winter conditions, neither MV nor HV was able to provide comfortable conditions with the given inflow parameters. However, a higher heating efficiency could be observed for the novel ventilation concept. To improve the thermal comfort for heating cases, the air inlet configuration as well as the air inlet temperatures have to be modified. During spring/fall and summer conditions, HV performs quite well regarding the thermal comfort despite the large temperature stratifications observed by the local air temperature sensors. For the spring/fall case, MV reveals uncomfortable equivalent temperatures in the upper cabin, resulting from the high amount of forced convection. However, MV shines out as an efficient ventilation system for cooling the car cabin.
In conclusion, both investigated ventilation systems offer advantages and disadvantages addressing the thermal comfort and the ventilation efficiency. For assessing the thermal comfort, the acquisition of equivalent temperatures is useful, since temperature and velocity probes only allow for an insufficient evaluation of comfortable thermal conditions inside a car cabin. In general, MV reveals mainly comfortable temperature stratifications, however, lower equivalent temperatures at the upper body can be detected. HV is characteristic for comfortable equivalent temperatures under spring/fall and summer conditions, although the temperature stratifications near the TPDs are significantly higher than those in MV. Both ventilation concepts have the potential for an efficient use of energy for ventilating a car cabin. MV shines out with a better cooling efficiency, whereas HV is more efficient for heating the car cabin. However, the results also show that an efficient operational mode of the ventilation system is prone to deficiencies regarding the thermal comfort. These can presumably be addressed by variations of the volume flow distribution and air inlet temperatures, especially for HV case. Besides the objective evaluation of the thermal conditions, trials with test persons would provide the opportunity for a subjective assessment of the thermal comfort.

# References


[1] A. Frohner et.al., *Novel heating concept for full electric vehicles*, Elektrotechnik & Informationstechnik, 132/2(2015), 168-171.

[2] J. Bosbach et.al., *Alternative ventilation concepts for aircraft cabins*, CEAS Aeronaut. J., 4(3), (2013), 301-313.

[3] T. Dehne et.al., *Experimental analysis of different ventilation concepts for the passenger compartment of a generic car*, $14^{th}$ Indoor Air Conference, Ghent, Belgium, July 3-8, (2016).

[4] M. Konstantinov and C. Wagner, *Numerical simulation of the thermal comfort in a model of a passenger car cabin*, $19^{th}$ DGLR/STAB-Symposium, Munich, ISSN 1612-2909, 132(2016), 383-393.

[5] *Heraeus*, https://www.heraeus.com/media/media/group/doc_group/products_1/hst/m_sensors/en_10/m_222_e.pdf, accessed on 2017-06-01.

[6] *Dantec Dynamics*, https://www.dantecdynamics.com/docs/products-and-services/thermal-comfort/PI264_ComfortSense.pdf, accessed on 2017-06-01.

[7] DIN EN ISO 14505-2, *Ergonomics of the thermal environment - Evaluation of thermal environments in vehicles - Part2: Determination of equivalent temperature*, International Standardization Organization, (2006).

[8] H. Han, *Ventilation effectiveness measurements using tracer gas technique*, Fluid Dynamics, Computational Modeling an Application. InTech, ISBN 978-953-51-0052-2, Chapter 3, 41-66, 2012.

[9] A. Wessling et.al., *Measurement System for Air Change Effectiveness in Car Cabins*, FISITA 2014 World Automotive Congress, Maastricht, Netherlands, June 2-6, (2014).

[10] Y. Zhang, *Indoor Air Quality Engineering*, ISBN 1-56670-674-2, Washington, CRC Press LLC, 2005.

[11] ASHRAE, *ASHRAE Handbook of Fundamentals*, American Society of Heating, Refrigerating and Air Conditioning Engineers, Inc., Atlanta, USA, (2001).

## Authors

Pascal Lange, M.Eng.: Received his master degree in mechanical engineering at the HTWK Leipzig, Germany in 2016. Title of his thesis was: “Experimental investigation of ventilation efficiency and thermal comfort of novel ventilation concepts in a car cabin”. He is working as research associate at the German Aerospace Center. Main topics are experimental investigation of ventilation efficiency and thermal comfort of novel ventilation concepts in a car cabin.

Dr. rer. nat. Daniel Schmeling: Received his Dr. title in physics at the Georg-August University in Göttingen, Germany in 2014. Title of the thesis was: “Experimental acquisition and characterization of large-scale flow structures in turbulent mixed convection”. He is working as research associate at the German Aerospace Center. Main topics are experimental investigations of ventilation and thermal comfort in train compartments and cars, fundamental research of thermal convection and development of measurement techniques in this field.

Tobias Dehne, M.Eng.: Received his master degree in electrical engineering at the HAWK Göttingen, Germany in 2012. Title of his thesis was: “Novel displacement ventilation systems for aircraft cabins”. He is working as technical employee at the German Aerospace Center. Main topics are the application of optical measurement techniques, such as Particle Image Velocimetry (PIV) and Infrared Thermography as well as classical measurement methods to mixed convective air flows in car and aircraft cabins of grounded based test facilities as well as in flight tests.

Dr. Ing. habil. Mikhail Konstantinov: Received his Dr. title in mechanical engineering at the Institute of Hydromechanics Ac. Sci. of Ukraine in 1984 and Dr. habil in Fluid dynamics at the University of Magdeburg in 1995. Title of the thesis was: “Interaction of vortex rings and vortex pairs”. He is working as research associate at the German Aerospace Center. Main topics are numerical simulations of thermal comfort in aircraft, train and passenger car compartments as well as coupling of flow simulations with comfort models and radiation solvers.

Dr. rer. nat. Johannes Bosbach: Received his Dr. title in physics at the University of Kassel, Germany in 2002. Title of the thesis was: “Ultrafast electron dynamics in metallic nanoparticles: the dephasing time of the surface plasmon”. He is working as team leader and principal investigator at the German Aerospace Center in Göttingen. Main fields of interest are indoor air flow and environmental control of aircraft as well as vehicle compartments, thermal convection and optical measurement techniques.